Fuel 212 (2018) 437–447

Contents lists available at ScienceDirect

Fuel

journal homepage: www.elsevier.com/locate/fuel

Full Length Article

Modeling study of residence time of molten slag on the wall in an entrained flow gasifier

Binbin Zhang[a,b], Zhongjie Shen[a,b], Qinfeng Liang[a,b,c], Jianliang Xu[a,b], Haifeng Liu[a,b,*]

[a] Key Laboratory of Coal Gasification and Energy Chemical Engineering of Ministry of Education, East China University of Science and Technology, P.O. Box 272, Shanghai 200237, PR China

[b] Shanghai Engineering Research Center of Coal Gasification, East China University of Science and Technology, P.O. Box 272, Shanghai 200237, PR China

[c] State Key Laboratory of Coal Conversion, Institute of Coal Chemistry, Chinese Academy of Sciences, PR China

ARTICLE INFO

Keywords:
Gasification
Coal slag
Residence time
Flow model

ABSTRACT

In an entrained flow coal gasifier, the slag viscosity property is of great importance to the slagging process. The slag viscosity is affected by the crystal mineral and the crystallization process has a time effect. The molten slag residence time in gasifier was calculated by slag flow model to estimate the isothermal time or crystal growth time during the cooling process. The residence times of tracer slag unit were calculated by the slag velocity. The residence time distribution (RTD) curve was obtained and the mean residence time was about 100–500 s in this study. Moreover, the molten slag mean residence time decreases significantly with increasing ash contents in coal, decreases slightly with increasing operating temperatures, and increases with increasing slag critical viscosities and temperatures. In addition, a plug flow reactor (PFR) series a similar laminar flow tubular reactor model was used to analysis the RTD curves of molten slag with different operating conditions.

1. Introduction

The entrained flow gasification is considered as a promising technology in coal conversion and widely used in industries of chemical and energy [1]. During the coal gasification, most of coal particles and fly ashes deposit on the wall, form slag layer which can protect the metal materials from the high temperature corrosion [2]. The molten slag flow down along the wall to the gasifier chamber outlet [3]. Therefore, the slag properties are crucial to the stable operation of gasifier due to the blocking slag and wall erosion problem [4].

The coal slag properties mainly include slag flowability, rheology, fusibility, and viscosity-temperature characteristics. The slag viscosity can be measured by the high-temperature rotational viscometer, and also can be predicted by different viscosity models [5–10]. The researchers found that the main factors which affected slag viscosity were temperature and the crystal minerals [11–13]. Kim and Oh [11] studied the formation of a crystalline phase and found it affected the slag viscosity in a Texaco gasifier. Moreover, the slag phase transition process was also closely related to crystal growth [14,15]. Yuan et al. [16] found that the liquid slag viscosity increased drastically when the crystalline phase accounted for 15.15–33.82%. Thus the crystallization characteristics of coal slag are of important to the slag viscosity and phase transition. Shen et al. [17,18] studied the crystallization behavior of coal slag during isothermal molten process in high-temperature stage microscopy, and found that the crystal size in molten slag first increased and then remained unchanged with increasing isothermal time. Xuan et al. [19–21] found that the crystallization ratio rate was high in the low temperature region, but in the high temperature region it was slow and required some incubation time to complete the process. Bai et al. [22] found that the residence time of coal ash at high-temperature had significant influence on the coal ash composition while little affected the amount of unburned carbon. During the cooling process of molten slag, the Temperature Time Transformation (TTT) diagram of slag was frequently used to study the slag properties, and the results were often related to time [23–26]. The above study indicated that the isothermal time during the cooling process had significant effect on the slag phase transition and the crystallization process. In a gasifier, the isothermal time during the cooling process corresponding to the residence time of molten slag on the wall. Therefore, understanding the residence time of molten slag on the wall has great meanings.

Understanding the slag flow properties is a prerequisite for study the residence time of molten slag. Experiment study for slag flow on the wall in an industrial gasifier is difficult due to the high temperature and pressure environment [27]. Hosseini and Gupta [28] used a vertical drop-tube furnace to study the ash deposition and slag formation with the effect of operating conditions and particle trajectory. Liang et al.

* Corresponding author at: Key Laboratory of Coal Gasification and Energy Chemical Engineering of Ministry of Education, East China University of Science and Technology, P. O. Box 272, Shanghai 200237, PR China.
E-mail address: hfliu@ecust.edu.cn (H. Liu).

http://dx.doi.org/10.1016/j.fuel.2017.10.073
Received 15 July 2017; Received in revised form 9 October 2017; Accepted 14 October 2017
Available online 23 October 2017

Nomenclature

a	model parameter
c	slag specific heat capacity
D	gasifier diameter (m)
g	gravitational constant (m/s^2)
h	height of slag cell (m)
H	slag cell position from the bottom of gasifier (m)
L	characteristic length (m)
m_{ex}	vertical outlet slag mass flow rate per unit (kg/s)
m_{in}	mass flow of particle deposition per unit (kg/s)
q_{in}	heat flux to the slag surface (W/m^2)
q_{out}	heat flux from the slag to the refractory layer (W/m^2)
Re	Reynolds number
n	model parameter
t	the overall flow time (s)
t_{min}	minimum residence time (s)
t_{res}	the residence time (s)
T_0	temperature of slag interface (K)
T_{cv}	temperature of critical viscosity (K)
T_g	gas temperature near wall (K)
u	slag velocity at distance x from slag-gas interface (m/s)
x	the distance from the slag-gas interface (m)
y	the distance from the gasifier top (m)

Greek letters

δ_l	thickness of liquid slag layer (m)
ε	emissivity
θ	slant angle of the wall (°)
μ_l	liquid slag viscosity (Pa s)
ρ	slag density (kg/m^3)
σ	blackbody radiation coefficient (W/m^2 K^4)
τ	the mean residence time of molten slag
τ_0	the correction time (s)
τ_l	the mean residence time of laminar flow reactor (s)
τ_p	the residence time of PFR (s)

Subscript

0	slag surface or x = 0
cv	critical viscosity
ex	out of the slag unit
f	slag flow
i	slag unit at horizontal direction
j	slag unit at vertical direction
in	inflow to the slag
l	liquid slag
res	residence time

[29] studied the slag deposition and heat flux in a pulverized coal entrained flow gasifier with the combination of pilot trial results and model method. The slag flow behavior in gasifier was mainly obtained by the simulation and modeling method. Seggiani [30] had built a simplified model to study the time varying slag flow and heat transfer in a Prenflo entrained flow gasifier, which was widely used in many studies [31,32]. The author assumed that the temperature profile in liquid slag was linear, and defined the temperature of critical viscosity (T_{cv}) as the transition temperature of liquid and solid slag layers. Thus the analytic equations of slag velocity and flow rate were obtained by the three conservation equation. Ye and Ryu [33,34] built a slag flow model with discretization to predict the thickness, velocity and temperature of the slag layer, the deposited slag was considered as a new control cell which attached to the original cell during the model construction. The model proposed by Yong et al. [35,36] was used in solid fuel gasification and combustion, in which the temperature profile of liquid was modified as cubic polynomial instead of linear. Furthermore the shear stress at the slag surface was considered in the momentum conservation equation. Zhang et al. [32] studied the slag flow and heat transfer properties with the effect of bubbles inside slag, and found it closer to industrial results after modified by the bubbles.

The modified model was based on Seggiani's [30] work to study the slag velocity and residence time distribution with modeling analyzed method in an entrained flow gasifier. From the results, the liquid slag velocity and residence time in different axial position was obtained. The molten slag residence time distribution (RTD) function and the RTD density function were also obtained during the model calculation. In addition, different operating conditions were used to study the molten slag RTD curves and mean residence times.

2. Model description

2.1. Slag flow models and governing equations

The slag flow model was established according to the method proposed by Seggiani [30]. The solid slag layer thickness is far less than the wall height, thus the liquid slag layer is considered as the vertical downward flow in a smooth vertical surface. Fig. 1 shows the schematic diagram cross section of liquid slag layer along the solid slag layer in an entrained flow gasifier. The Reynolds number of liquid slag can be calculated as follows:

$$Re = \frac{\rho u L}{\mu_l} \tag{1}$$

where Re is the Reynolds number of liquid slag, ρ is the liquid slag density, u is the liquid slag velocity, μ_l is the liquid slag viscosity, L is the characteristic length. In this study, the liquid slag density is 2830 kg/m^3, the characteristic length is the wall height, which is 7 m. According to the previous studies [32], the fastest velocity of liquid slag is less than 5 cm/s, and the smallest viscosity of liquid slag is more than 0.5 Pa s. Therefore, the largest Reynolds number of liquid slag is less than 2000. Based on the Reynolds number, the liquid slag is considered as laminar flow. As shown in Fig. 1, the planar space of the liquid slag is

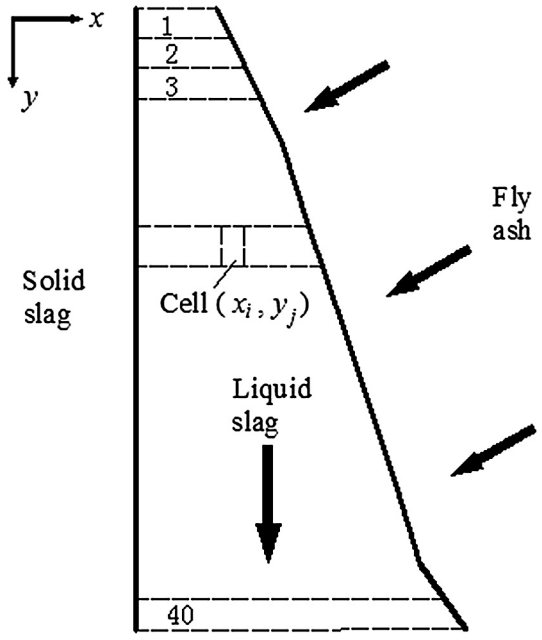

Fig. 1. Schematic diagram cross section of liquid slag layer.

uniformly separated into 40 layers along the y axis direction, and each layer is divided into several cells along the x axis direction.

According to the Seggiani's [30] method, the mass conservation equations for the y_j layer in the steady-state condition can be express as:

$$m_{in,j} + m_{ex,j-1} - m_{ex,j} = 0 \tag{2}$$

The incoming slag mass flow rate in first layer ($j = 0$) is 0, the mass flow rate of particle deposition in each layer is known from the CFD modeling, therefore the leaving slag mass flow rate in y_j layer can be calculated by superposition method with Eq. (2). Moreover, the leaving slag mass flow rate of y_j layer can also be expressed as follow:

$$m_{ex,j} = \rho\pi D_j \int_0^{\delta_{l,j}} u_j dx \tag{3}$$

The momentum conservation for the y_j layer can be expressed as follow:

$$\frac{d}{dx_j}\left(\mu_{l,j}\frac{du_j}{dx_j}\right) = -\rho g\cos\theta_j, \quad \begin{matrix} x_j = 0, \mu_{l,j}\frac{du_j}{dx_j} = 0 \\ x_j = \delta_{l,j}, u_j = 0 \end{matrix} \tag{4}$$

where the liquid slag viscosity is considered as an exponential function of the temperature. Combining with the assumption that the slag temperature is linear distribution, the liquid slag viscosity changing with the position can be expressed as:

$$\mu(x)_j = \mu(0)_j \exp\left(\frac{\ln(\mu(\delta_{l,j})_j/\mu(0)_j)}{\delta_{l,j}} x_j\right) \tag{5}$$

Substituting Eq. (5) into Eq. (4), the liquid slag velocity along x axis is obtained by the direct integration.

$$u(x)_j = \frac{\rho g\cos\theta_j \delta_{1,j}^2}{\mu(0)_j}\left[e^{\alpha_j}\left(\frac{1}{\alpha_j} - \frac{1}{\alpha_j^2}\right) - e^{\frac{\alpha_j x_j}{\delta_{l,j}}}\left(\frac{x_j}{\alpha_j \delta_{l,j}} - \frac{1}{\alpha_j^2}\right)\right] \tag{6}$$

where $\alpha = -\ln(\mu(\delta_l)/\mu(0))$, $\mu(0)$ is the slag viscosity at the gas-slag interface and $\mu(\delta_l)$ is the slag viscosity at the solid-liquid slag interface. Combining the Eqs. (2), (3) and (6), the liquid slag layer thickness in y_j layer is obtained. Thus the liquid slag velocity distribution at y_j layer is obtained by Eq. (6).

The energy conservation for the y_j layer can be expressed as follow:

$$m_{\mathrm{in,j}} C_s T_g + \frac{1}{2}(T_{\mathrm{o,j-1}} + T_{\mathrm{cv}}) m_{\mathrm{ex,j-1}} C_s - \frac{1}{2}(T_{\mathrm{o,j}} + T_{\mathrm{cv}}) m_{\mathrm{ex,j}} C_s - q_{\mathrm{out,j}} + q_{\mathrm{in,j}} = 0 \tag{7}$$

$$q_{\mathrm{in,j}} = h(T_{\mathrm{g,j}} - T_{\mathrm{o,j}}) + \varepsilon\sigma(T_{\mathrm{g,j}}^4 - T_{\mathrm{o,j}}^4) \tag{8}$$

The first slag layer is divided into N_1 cells. The second slag layer is divided into $(N_1 + N_2)$ cells due to slag deposition from the side. According to the assumption of laminar flow, the first N_1 cells of the second layer are streaming down from the upper layer. The third slag layer is divided into $(N_1 + N_2 + N_3)$ cells, and so on. According to the tracing method, we define that each slag cell that has just deposited on the wall as the tracer unit. To ensure the amount of tracer unit unchanged, the cells between adjacent two layers have the following relationship:

$$m_{ex,i,j-1} = m_{ex,i,j} \tag{9}$$

The mass flow rate of cell (i, j) can be calculated as follows:

$$m_{ex,i,j} = \rho\pi D_j \int_{x_{i-1}}^{x_i} u_j dx \tag{10}$$

After that the liquid slag thickness in each layer is obtained, the thicknesses of the cells in first layer are defined as the initial data. The thicknesses of the first N_1 cells of second layer are calculated by the Eqs. (9) and (10), and the thicknesses of rest N_2 cells are defined as the initial data. And so on, the thicknesses of the cells in other layer are obtained.

Once the thicknesses of each slag cell are obtained, the average velocity of slag in cell (i, j) can be calculated as follows:

$$u_{ij} = \frac{1}{x_i - x_{i-1}} \cdot \int_{x_{i-1}}^{x_i} u(x)_j dx \tag{11}$$

The liquid slag is laminar flow and streaming down along the vertical direction. The slag will not mix between each layer under the laminar flow state. The residence time of slag in cell (i, j) is calculated as follows:

$$t_{res}(i,j) = h_{i,j}/u_{i,j} \tag{12}$$

where $h_{\mathrm{i,j}}$ is the height of cell (i, j) along y axis. Each slag unit is streaming down from the upper unit along the y axis. Therefore, the overall residence time of tracer slag unit is calculated as follows:

$$t_i = \sum_j t_{res}(i,j) \tag{13}$$

The residence time distribution function and density function of liquid slag is calculated as follows:

$$E(t) = \frac{m_{ex,i}}{(t_i - t_{i-1})\sum m_{ex,i}} \tag{14}$$

$$F(t) = \int_0^t E(t)dt \tag{15}$$

The mean residence time of the liquid slag on the wall is a significant characteristic for the slag residence time distribution, which is defined as:

$$\tau = \frac{\sum t_i m_{ex,i}}{\sum m_{ex,i}} \tag{16}$$

The mean residence time of liquid slag on the wall can be used to evaluate the slag isothermal time or residence time during the cooling process.

2.2. Simulation conditions and methods

The slag flow and transfer model is tested in a Shell pulverized coal gasifier (2000 t/d coal consumption) with boundary conditions from CFD simulation. Fig. 2 shows the configuration and the dimensions of the gasifier. The CFD simulation process is based on the Xu's [37] method in reference. The chemical reactions in gasifier include homogeneous reaction and heterogeneous reaction. The homogeneous reactions are simulated by the eddy dissipative concept model and the heterogeneous reactions are simulated by random pore model. It is assumed that a reaction occurs in small turbulent structures and the

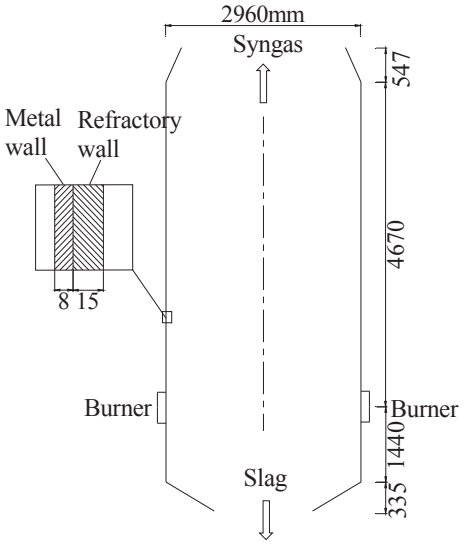

Fig. 2. Configuration and the dimensions of the Shell gasifier.

reactants are mixed at the molecular scale, the reaction rate is present by the Arrhenius equation when the time is longer. The realizable k-ε model is adopted to model the turbulence of gas phase. In addition, the particle motion is simulated by random trajectory model in Lagrangian coordinates. The particle sizes were a function of the char conversion, reaction regime and the effectiveness factors. The particle deposition mass rate distribution and the near-wall gas temperature distribution are modeling results from the 3-D CFD simulation results with the industrial gasifier data (under 50% load condition, operating temperature is 1432 ˚C and ash content of coal is 23 wt%), as shown in Fig. 3. The viscosity of coal slag is measured by a high-temperature rotational viscometer (Theta Industries, Port Wahington, NY). Moreover, we correct the error of viscosity data caused by the bubbles in slag according to the method in Ref. [32]. Thus the viscosity-temperature curve is obtained as shown in Fig. 4.

In addition, the temperature of critical viscosity (T_{cv}) is used as the transition temperature between the liquid and solid slag layers, as Seggiani's [30] assumption. In general, T_{cv} is defined as the temperature at which the viscosity rapid changes according to the Ref. [38]. Therefore, T_{cv} is obtained from the viscosity-temperature curve, which is corresponding to the point of mutational viscosity. From the viscosity-temperature curve of given slag as shown in Fig. 4, the critical temperature (T_{cv}) is 1344 ˚C and the critical viscosity (μ_{cv}) is 3.5 Pa s. In order to study the effect of operation conditions on liquid slag residence time distribution, we change the test single initial parameters in the case of keeping other conditions unchanged.

3. Results and discussion

3.1. The slag flow characteristic in different positions

Fig. 5 shows the slag thickness distribution along the wall in gasifier. The liquid slag thickness increases with the flow direction asshown in Fig. 5(a). Especially, the liquid slag thickness increases rapidly at the intersection of the vertical planeand conical surface (at positions about 0.5 m and 6.5 m from the top of gasifier), and the liquid slag thickness almost remain the same near the nozzle (at positions about 5 m from the top of gasifier). Because the particle deposition rate and the gas temperature are obvious fluctuation at this place, moreover, the liquid slag from the vertical plane impacts to the conical surface, which can cause instantaneous kinetic energy loss and velocity slow down. Fig. 5(b) shows the solid slag thickness distribution, the thickness is obviously thinner near the nozzle position and gasifier bottom cone. Fig. 6 shows the heat flux distribution of slag along the gasifier, which is calculated from energy equations. Under 50% load condition, the steam output of Shell pulverized coal gasifier can reach 15–18 t/h. Based on the value of steam output, the range of average heat flux of slag is 140–165 kW/m^2. Therefore, the calculated results are in accordance with the data of the industrial gasifier compared the heat flux.

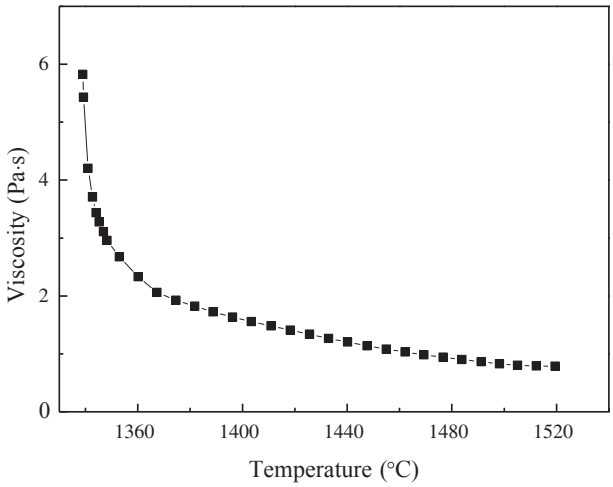

Fig. 4. Viscosity-temperature data of slag in gasifier.

The liquid slag velocity increases along the x axis direction as shown in Fig. 7(a). The liquid slag velocity is 0 at the liquid-olid slag interface according to the setting of boundary condition. On the contrary, the velocity reaches the maximum and almost no increases near the liquid slag surface. Fig. 7(b) shows the liquid slag average velocity distribution at different heights. The results illustrate that the liquid slag velocity increases along the slag flow direction until the bottom conical surface. The liquid slag velocity is decreased at the lower part of gasifier. The reason is the same as the previous analysis, the liquid slag impinging on the conical surface will cause the instantaneous kinetic energy loss.

According to the liquid slag velocity distribution in Fig. 7, the fastest velocity of liquid slag is less than 5 cm/s, and the smallest viscosity of liquid slag is more than 0.5 Pa s. Therefore, the largest Reynolds number of liquid slag is less than 2000. In this condition, the assumption that the liquid flow is laminar is reasonable.

3.2. The tracer slag unit residence time and flow rate

Fig. 8 shows the tracer slag unit residence time and flow rate distribution at the gasifier outlet according to Eqs. (11) and (13). From the tracer slag unit residence time distribution, it can be found which part of slag residence time is longer in gasifier before they are slagging. The tracer slag unit residence time decreases along the x axis direction, especially near the liquid-solid slag interface. The tracer slag unit residence time is the shortest at the liquid slag surface due to the highest velocity, and the shortest flow time is about 17 s. The tracer slag unit mass flow rate distribution at the gasifier chamber outlet is shown in Fig. 8(b). On the contrary, the tracer slag unit mass flow rate increases along the x axis direction. In a similar way, the tracer slag unit mass

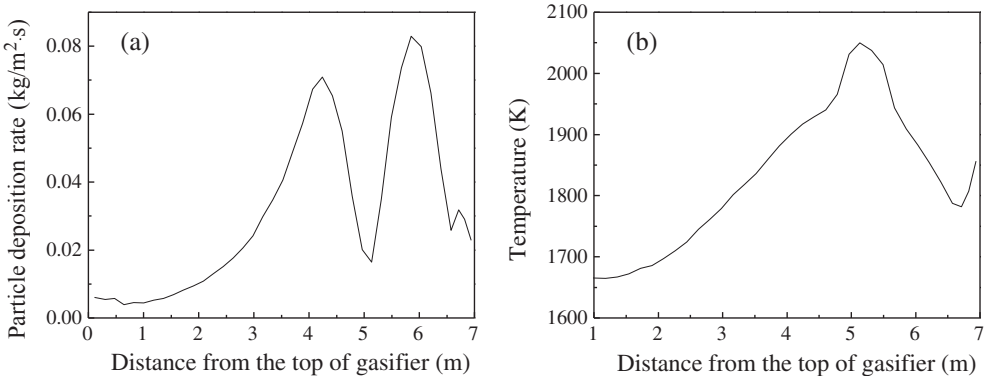

Fig. 3. Particle deposition rate and gas temperature distribution along the wall.

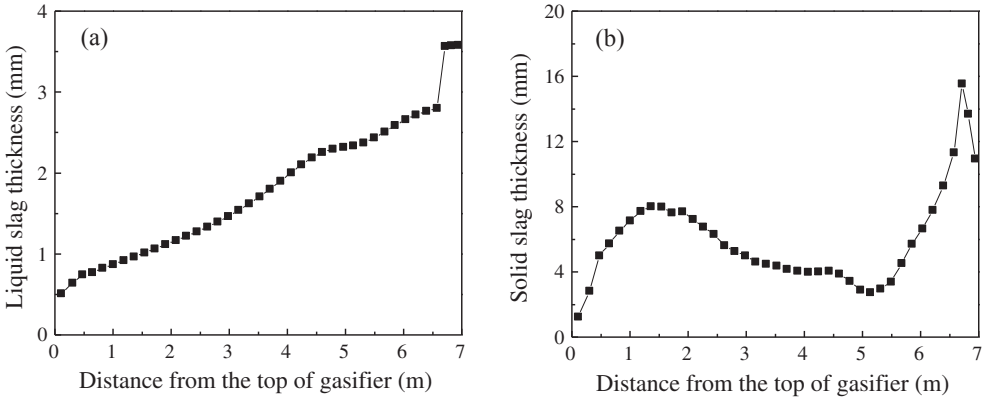

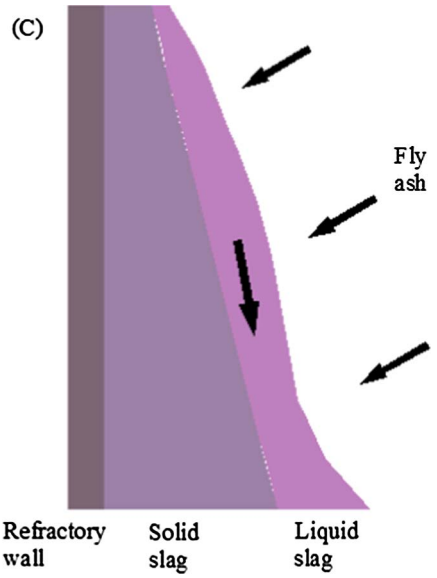

Fig. 5. Slag thickness distribution and diagram along the gasifier.

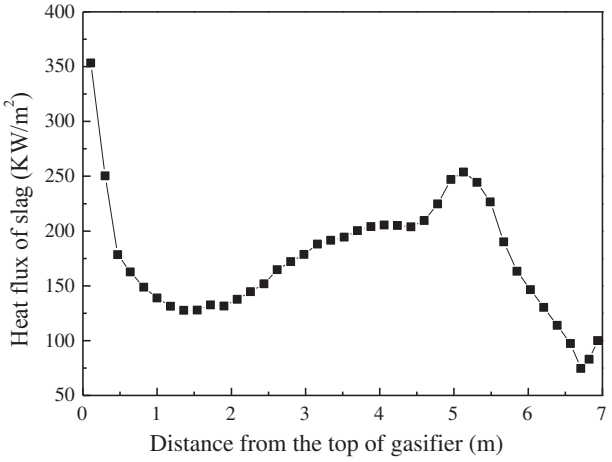

Fig. 6. Heat flux distribution of slag along the gasifier.

flow rate is the largest at the liquid slag surface due to the highest velocity.

3.3. The residence time distribution of molten slag on the wall

Fig. 9 shows the RTD function and density function of molten slag on the wall. In this paper, the entire liquid slag layer is treated as a reactor in steady state conditions. The reactor inlet is the liquid slag surface, which is corresponding to the interface of fly ash deposition. The reactor outlet is the slag discharge opening of the gasifier. According to the tracing method, the known dose of tracer slag is deposited from the chamber of the gasifier to the wall. The mass flow rate of tracer slag at the slag discharge opening can be calculated from the above section. Therefore, the residence time distribution of molten slag can be calculated according to the definition of tracing method. From the assumption that the liquid slag flow is laminar, the liquid slag flow on the wall is a non-ideal flow model because there is a gradient in velocity on the flow vertical plane. The mean residence time is 170 (s) which is calculated by the Eq. (16). It means the liquid slag needs to flow and be cooled for average 170 (s) after they deposit on the wall.

3.4. The mean residence time with different operation condition

3.4.1. The mean residence time with different ash contents

The mean residence time of molten slag is a significant parameter for a gasifier. Fig. 10(a) shows the mean residence time of liquid slag on the wall with different ash contents in coal. On the basis of the previous calculations, the ash contents changes by 20% and 40% respectively in the case of keeping other conditions unchanged. We assume that the ash content will directly affect the particle deposition rate, thus the particle deposition mass rate distribution in Fig. 3(a) will change by percentage. Fig. 10(a) illustrates that the liquid slag mean residence time decreases with the increased ash content in coal. The increased ash content in coal will increase the particle deposition mass rate in each unit. From the definition of trace method, the increased particle

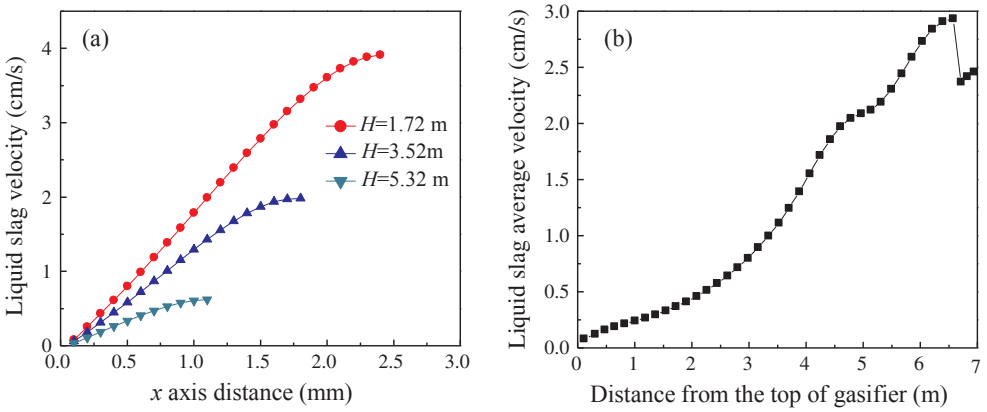

Fig. 7. Slag velocity distribution at different heights and average velocity along the gasifier.

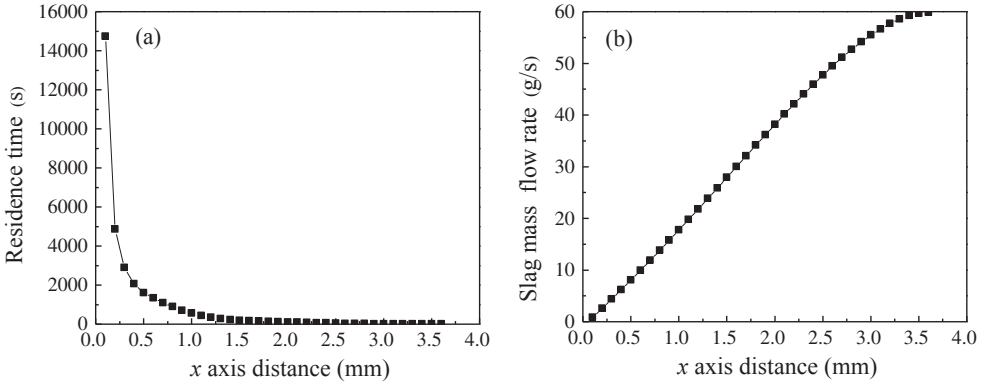

Fig. 8. The tracer slag unit residence time distribution and mass flow rate at the gasifier outlet.

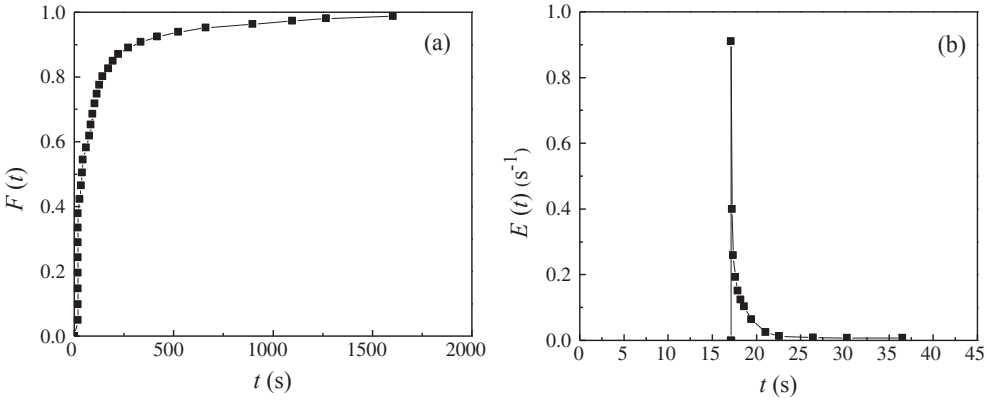

Fig. 9. The RTD function and RTD density function of molten slag.

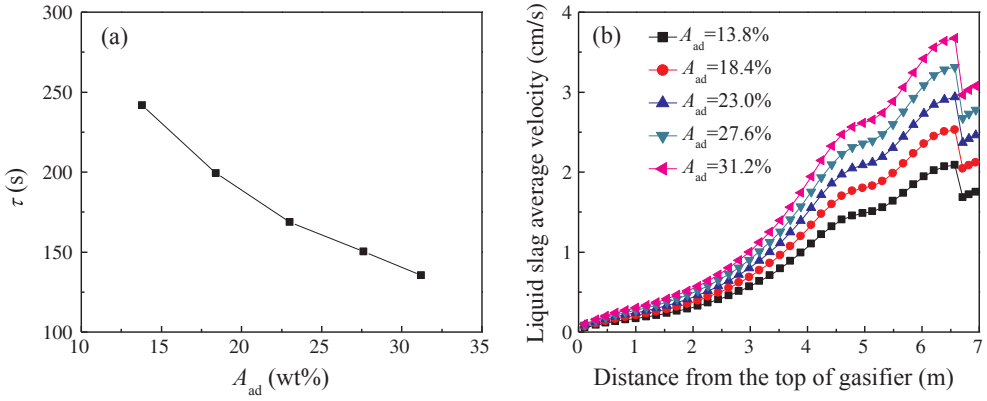

Fig. 10. The mean residence time and velocity distribution of molten slag with different ash contents.

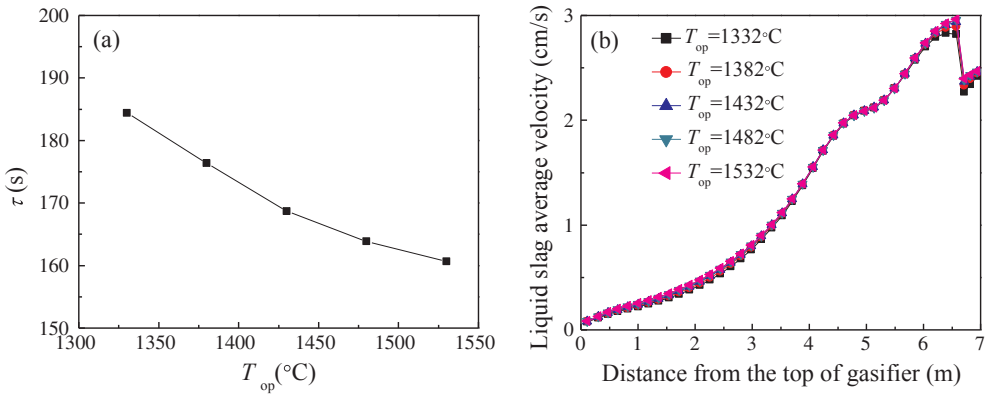

Fig. 11. The mean residence time and velocity distribution of molten slag with different operating temperatures.

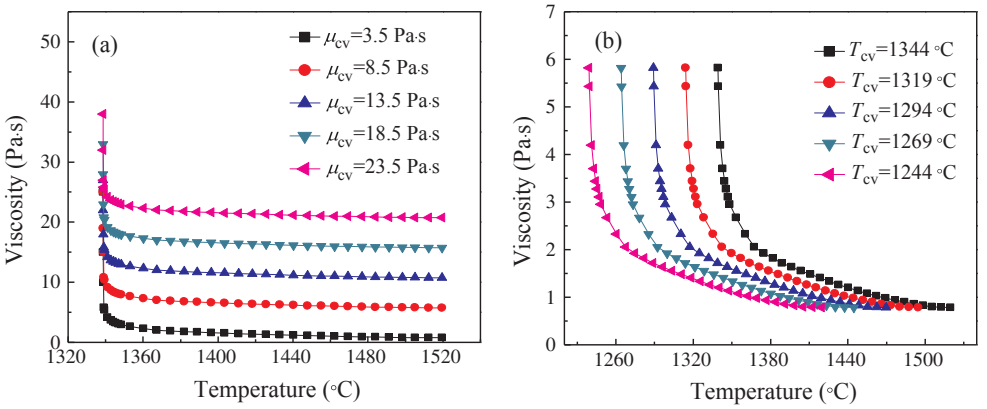

Fig. 12. Viscosity-temperature data of different slag types (a: T_{cv} = 1344 °C, b: μ_{cv} = 3.5 Pa s).

deposition mass rate will increase the amount of traced material at the reactor inlet. The amount of traced material at the reactor outlet will increase at the same time. It is difficult to determine the trend of change in liquid slag residence time. However, from the calculation process as shown in above section, the increased particle deposition mass rate will increase the liquid slag thickness and the velocity. The liquid slag average velocity increases with the increased ash content as shown in Fig. 10(b). And then, the increased liquid slag velocity will decrease the overall flow time of liquid slag, it means the liquid slag residence time decreases. The liquid slag mean residence time is reduced by about 22% when the ash content in coal increases 40%.

3.4.2. The mean residence time with different operating temperatures

Fig. 11(a) shows the mean residence time of liquid slag on the wall with different operating temperature in gasifier. On the basis of the previous calculations, the operating temperature changes by 50 and 100 (K) respectively in the case of keeping other conditions unchanged. We assume that the operating temperature will directly affect the gas temperature near the wall, thus the near-wall gas temperature distribution in Fig. 3(b) will change by the corresponded magnitude. Fig. 11(a) illustrate that the liquid slag mean residence time increases with the increased operating temperature in gasifier. The liquid slag mean residence time is reduced by about 4.8% when the operating temperature increases 100 K. It illustrates the liquid slag residence time is less affected by operating temperature. From the calculation process as shown in above section, the increased near-wall gas temperature will slightly increase the slag velocity in the gasifier as shown in Fig. 11(b). As a result, the liquid slag residence time will decrease in low amplitude.

3.4.3. The mean residence time with different slag types

To study the liquid slag residence time at different slag types, we assume the different slag viscosity-temperature curve as shown in Fig. 12. In order to ensure the unity of the variable, we assume the critical viscosity (μ_{cv}) and the temperature of the critical viscosity (T_{cv}) remain the same in two cases, respectively.

Fig. 13(a) shows the mean residence time of liquid slag on the wall with different slag critical viscosities. From the calculation process as shown in above section, the increased slag viscosity will obviously decrease the slag velocity as shown in Fig. 13(b). As a result, the increased slag viscosity will obviously increase the liquid slag residence time. The liquid slag mean residence time is increasing by about 98% when the critical viscosity increases 10 Pa s.

Fig. 14(a) shows the mean residence time of liquid slag on the wall with different slag critical temperatures. From the calculation process as shown in above section, the increased slag viscosity will decrease the slag velocity as shown in Fig. 14(b). As a result, the decreased slag viscosity will decrease the liquid slag residence time. The liquid slag mean residence time is reduced by about 8.5% when the temperature of critical viscosity increases 50 K. From the above results, the mean residence time of molten slag is mainly influenced by the slag critical viscosity instead of the critical temperature.

From the above model results, the molten slag residence time is mainly influenced by the slag viscosity and deposition rate. The great the slag viscosity, the slower the slag flow velocity, resulting a longer residence time. An increase in the amount of slag deposition will result an increase in slag flow mean velocity, thus resulting in a shorter residence time. In addition, the operating temperature and the slag critical temperature have little effect on molten slag residence time. In other word, the operating temperature and slag critical temperature affect the temperature on the both sides of liquid slag. From the model derivation, the effect of the slag temperature on slag thickness and velocity is not significant, thus the impact on slag residence time is small.

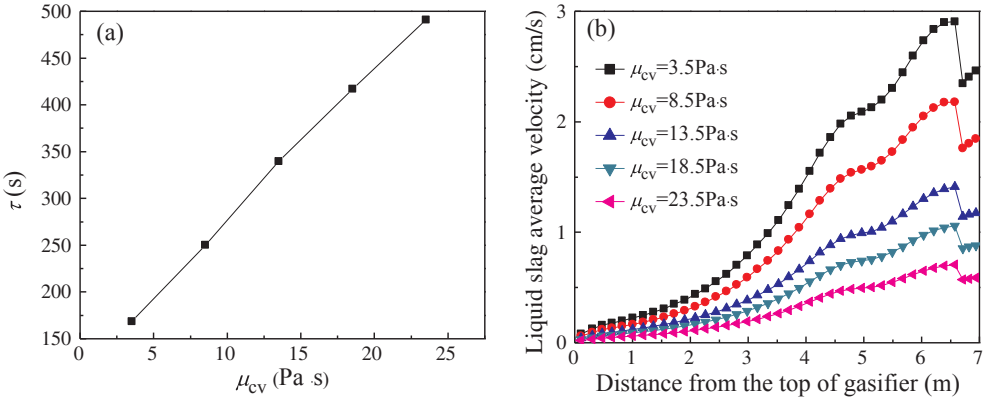

Fig. 13. The mean residence time and velocity distribution of molten slag with different slag critical viscosities.

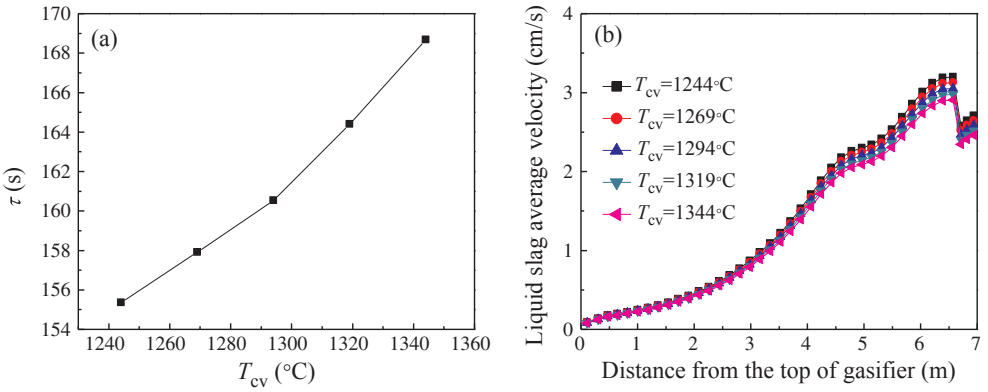

Fig. 14. The mean residence time and velocity distribution of molten slag with different slag critical temperatures.

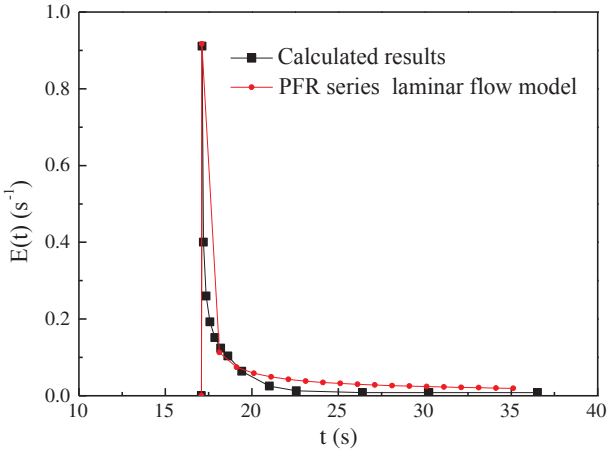

Fig. 15. The dimensionless RTD by the calculated results and laminar flow reactor model.

3.5. Model analysis of RTD curves

The RTD curves analysis is helpful for the studying of slag flow in gasifier. The molten slag flow process is a non-ideal flow, which can be simulated by a non-ideal reactor model. From the RTD curves of molten slag, the flow process can be approximated simulated by a plug flow reactor (PFR) series a laminar flow tubular reactor. The RTD function for a Newton fluid in a standard laminar flow tubular reactor is calculated by the follow equation [39]:

$$E(t) = 0, \qquad t < \tau_l/2$$
$$E(t) = \tau_l^2/2t^3, \quad t \geqslant \tau_l/2 \tag{17}$$

where τ_l is the mean residence time of laminar flow tubular reactor.

However, the molten slag flow process does not fully comply with a standard laminar flow tubular reactor. In this study, the flow velocity is variable in the axial direction and the position of the reactor feed entrance point is also changed with direction of flow. Therefore, a PFR series a similar laminar flow reactor model with some parameters is adopted as follow:

$$E(t) = 0, \qquad t < \tau_p$$
$$E(t) = \frac{(\tau_p)^{n-1}}{a(t-\tau_0)^n}, \quad t \geqslant \tau_p \tag{18}$$

where τ_p is the residence time of PFR, τ_0 is the correction time, a and n is the model parameter. The RTD curve in Fig. 9(b) is fitted by Eq. (18) and the fitting result is shown in Fig. 15, thus the model parameters is obtained as: $\tau_p = 17.12$ s, $\tau_0 = 17.08$ s, $a = 2.91$, $n = 0.62$.

In the previous section, we have study the RTD of molten slag in different operating conditions. Therefore, the dependence on the adjusted parameters on operating conditions is presented in Figs. 16–19.

Different operating conditions results in different molten slag RTD curves, thus resulting in different model parameters. The model parameters change linearly with mostly of the operating conditions except the operating temperature. The reason is that the operating temperature affects the slag viscosities with non-linear law, thus the slag velocity and residence time are also non-linear change. From the Figs. 16–19, the residence time of PFR decreases with the increasing ash contents of coal and operating temperatures, while increases with the increasing critical viscosities and critical temperatures. In addition, the model analysis of RTD curves is an approximation processing method. The actual RTD curves of molten slag should be measured according to the experiment method or calculated by a numerical method.

4. Conclusion

The residence time distribution of molten slag on the wall in gasifier was studied by the modeling method. The molten slag thickness and

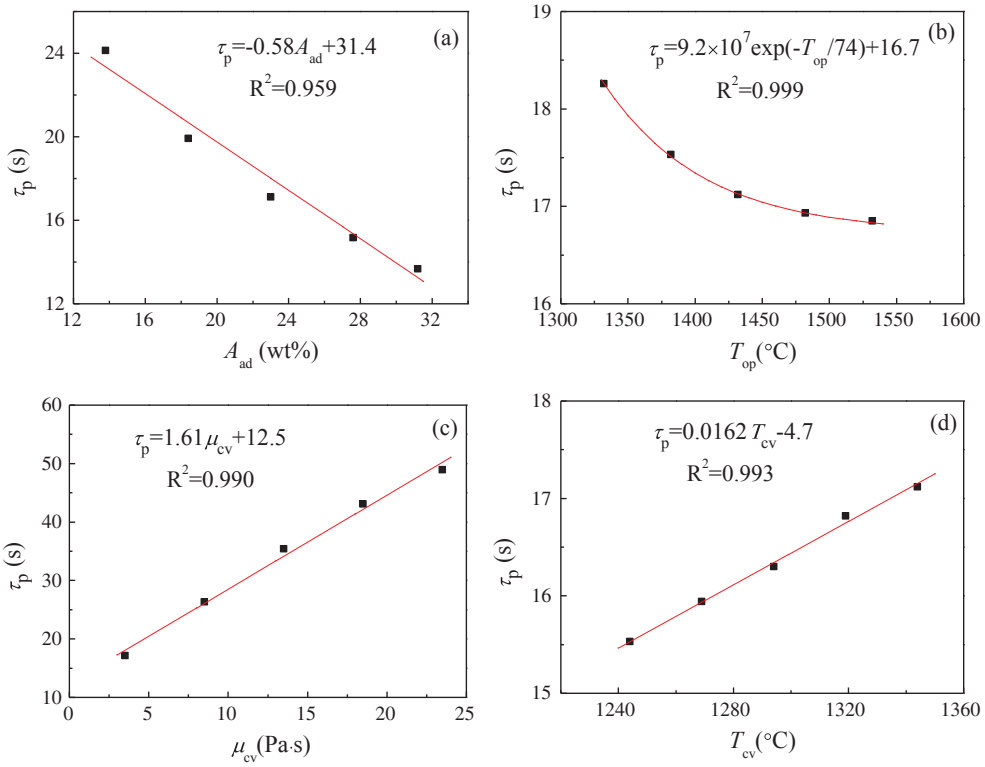

Fig. 16. Adjusted parameter τ_p affected by operating conditions (a: ash content of coal; b: operating temperature; c: slag critical viscosity; d: slag critical temperature) and fitting relationship.

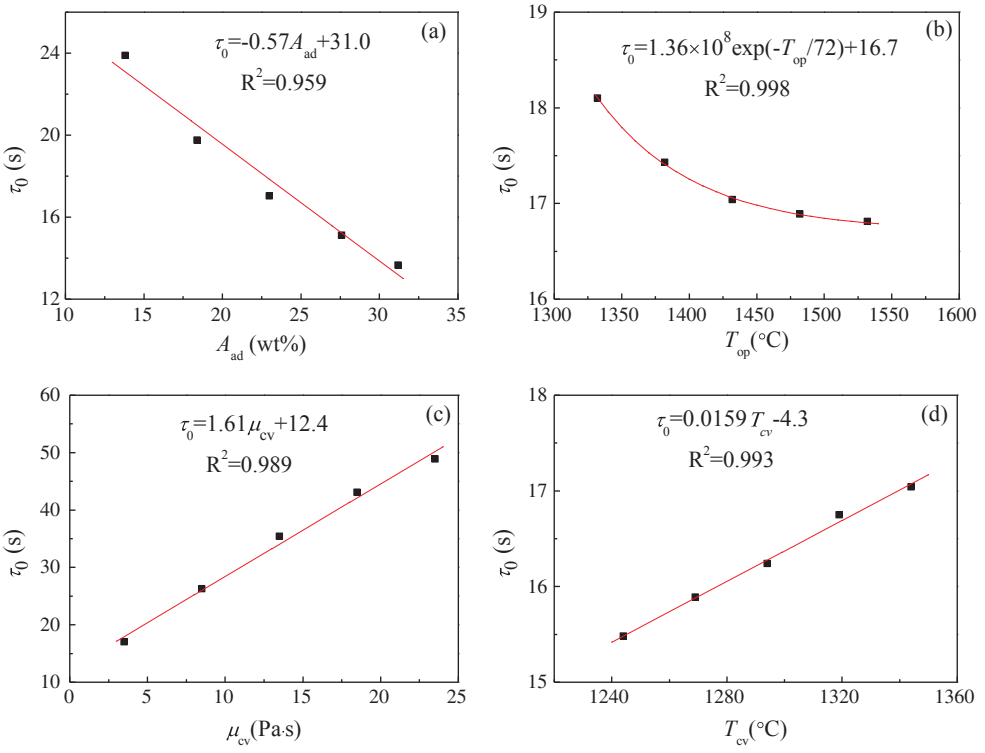

Fig. 17. Adjusted parameter τ_0 affected by operating conditions (a: ash content of coal; b: operating temperature; c: slag critical viscosity; d: slag critical temperature) and fitting relationship.

velocity distribution were obtained with the slag flow model. The residence times of tracer slag unit were calculated by the slag velocity distribution in each layer. From the model results, the RTD curve is obtained and the mean residence time of molten slag in this study is about 100–500 s. Moreover, the molten slag mean residence time decreases significantly with the increase of ash content in coal. As the operating temperature increases, the molten slag residence time decreases slightly. The molten slag mean residence time increases with the increase of slag critical viscosities and critical temperatures. In addition, a PFR series a similar laminar flow tubular reactor model is used to analysis the RTD curves of molten slag. The residence time of PFR in the model decreases with increasing ash contents and operating temperature, while increases with increasing slag critical viscosities and critical temperatures.

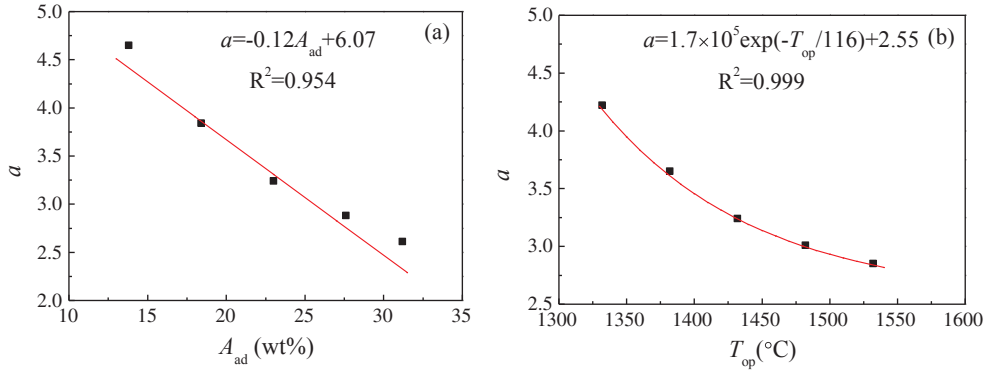

Fig. 18. Adjusted parameter *a* affected by operating conditions (a: ash content of coal; b: operating temperature; c: slag critical viscosity; d: slag critical temperature) and fitting relationship.

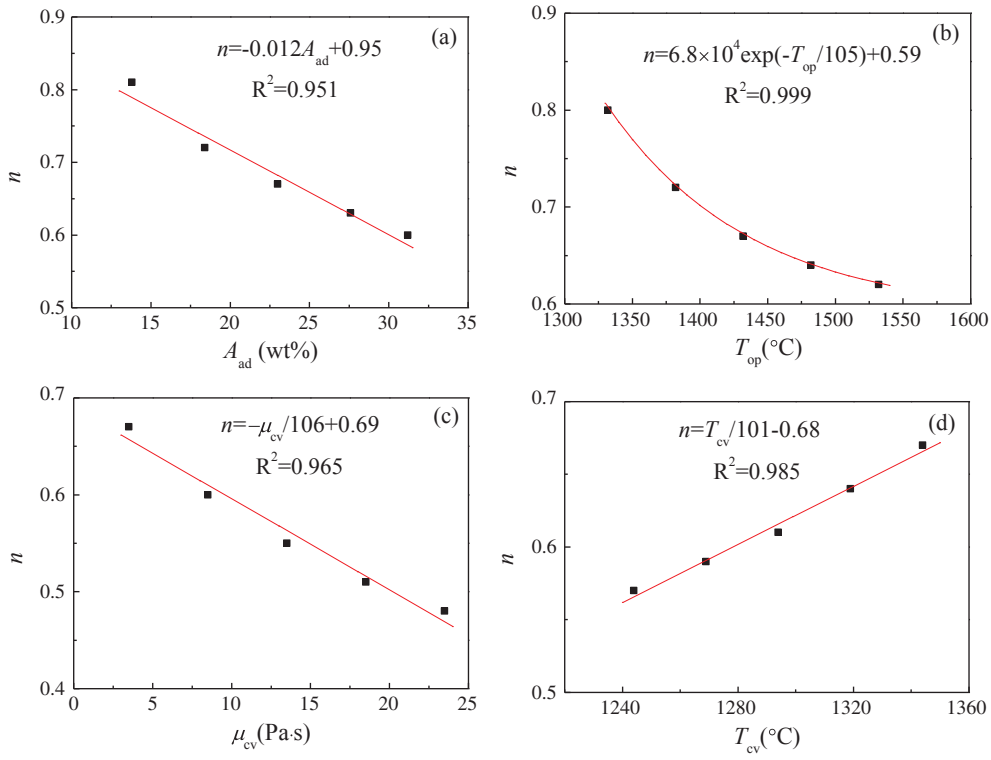

Fig. 19. Adjusted parameter *n* affected by operating conditions (a: ash content of coal; b: operating temperature; c: slag critical viscosity; d: slag critical temperature) and fitting relationship.

Acknowledgement

This study was supported by the Foundation of Shanghai Science and Technology Committee (14dz1200100), the National Natural Science Foundation of China (U1402272), the National Natural Science Foundation of China (21376082), and the Foundation of State Key Laboratory of Coal Conversion (Grant No. J16-17-301).

References

[1] Gong Y, Yu GS, Guo QH, Zhou ZJ, Wang FC, Liu YD. Pilot-scale comparison investigation of different entrained-flow gasification technologies. Chem Eng Sci 2015;138:291–302.
[2] Xuan WW, Zhang JS, Xia DH. Crystallization characteristics of a coal slag and influence of crystals on the sharp increase of viscosity. Fuel 2016;176:102–9.
[3] Xu JL, Dai ZH, Liu HF, Guo LY, Sun F. Modeling of multiphase reaction and slag flow in single-burner coal water slurry gasifier. Chem Eng Sci 2017;162:41–52.

[4] Kurowski MP, Spliethoff H. Deposition and slagging in an entrained-flow gasifier with focus on heat transfer, reactor design and flow dynamics with SPH. Fuel Process Technol 2016;152:147–55.
[5] Buhre BJP, Browing GJ, Gupta RP, Wall TF. Measurement of the viscosity of coal-derived slag using thermomechanical analysis. Energy Fuels 2005;19(3):1078–83.
[6] Browning GJ, Bryant GW, Hurst HJ, Lucas JA, Wall TF. An empirical method for the prediction of coal ash slag viscosity. Energy Fuels 2003;17(3):731–7.
[7] Duchesne MA, Macchi A, Lu DY, Hughes RW, McCalden D, Anthony EJ. Artificial neural network model to predict slag viscosity over a broad range of temperatures and slag compositions. Fuel Process Technol 2010;91(8):831–6.
[8] Duchesne MA, Bronsch AM, Hughes RW, Msset PJ. Slag viscosity modeling toolbox. Fuel 2013;114:38–43.
[9] Van Dyk JC, Waanders FB, Benson SA, Laumb ML, Hack K. Viscosity predictions of the slag composition of gasified coal, utilizing factsage equilibrium modeling. Fuel 2009;88(1):67–74.
[10] Van Dyk JC, Benson SA, Laumb ML, Waanders B. Coal and coal ash characteristics to understand mineral transformations and slag formation. Fuel 2009;88(6):1057–63.
[11] Kim Y, Oh MS. Effect of cooling rate and alumina dissolution on the determination of temperature of critical viscosity of molten slag. Fuel Process Technol 2010;91(8):853–8.
[12] Matjie RH, French D, Ward CR, Pistorius PC, Li ZS. Behaviour of coal mineral matter in sintering and slagging of ash during the gasification process. Fuel Process Technol 2011;92:1426–33.
[13] Ilyushechkin AY, Hla SS, Roberts DG, Kinaev NN. The effect of solids and phase compositions on viscosity behaviour and T-CV of slags from Australian bituminous coals. J Non-Cryst Solids 2011;357(3):893–902.
[14] Kalmanovitch DP, Williamson J. Crystallization of coal ash melts. J Am Chem Soc 1986;301:234–55.
[15] Nowok JW. Viscosity and phase transformation in coal ash slags near and below the temperature of critical viscosity. Energy Fuels 1994;8(6):1324–36.
[16] Yuan HP, Liang QF, Gong X. Crystallization of coal ash slags at high temperatures and effects on the viscosity. Energy Fuels 2012;26:3717–22.
[17] Shen ZJ, Liang QF, Zhang BB, Xu JL, Liu HF. Effect of continuous cooling on the crystallization process and crystal compositions of iron-rich coal slag. Energy Fuels 2015;29:3640–8.
[18] Shen ZJ, Hua X, Liang QF, Xu JL, Han D, Liu HF. Reaction, crystallization and element migration in coal slag melt during isothermal molten process. Fuel 2017;191:221–9.
[19] Xuan WW, Whitty KJ, Guan QL, Bi DP, Zhang JS. Influence of isothermal temperature and cooling rates on crystallization characteristics of a synthetic coal slag. Fuel 2014;137:193–9.
[20] Xuan WW, Whitty KJ, Guan QL, Bi DP, Zhan ZH, Zhang JS. Influence of Fe2O3 and atmosphere on crystallization characteristics of synthetic coal slags. Energy Fuels 2015;29:405–12.
[21] Xuan WW, Whitty KJ, Guan QL, Bi DP, Zhan ZH, Zhang JS. Influence of SiO2/Al2O3 on crystallization characteristics of synthetic coal slags. Fuel 2015;144:103–10.
[22] Bai J, Li W, Li BQ. Characterization of low-temperature coal ash behaviors at high temperatures under reducing atmosphere. Fuel 2008;87(4–5):583–91.
[23] Kashiwaya Y, Cicutti CE, Cramb AW. An investigation of the crystallization of a continuous casting mold slag using the single hot thermocouple technique. ISIJ Int 1998;38(4):357–65.
[24] Kashiwaya Y, Nakauchi T, Pham KS, Akiyama S, Ishii K. Crystallization behaviors concerned with TTT and CCT diagrams of blast furnace slag using hot thermocouple technique. ISIJ Int 2007;47(1):44–52.
[25] Wen GH, Liu H, Tang P. CCT and TTT diagrams to characterize crystallization behavior of mold fluxes. J Iron Steel Res Int 2008;15(4):32–7.
[26] Li J, Wang XD, Zhang ZT. Crystallization behavior of rutile in the synthesized ti-bearing blast furnace slag using single hot thermocouple technique. ISIJ Int 2011;51(9):1396–402.
[27] Wang J, Liu HF, Liang QF, Xu JL. Experimental and numerical study on slag deposition and growth at the slag tap hole. Fuel Process Technol 2013;106:704–11.
[28] Hossein S, Gupta R. Inorganic matter behavior during coal gasification: effect of operating conditions and particle trajectory on ash deposition and slag formation. Energy Fuels 2015;29:1503–19.
[29] Liang QF, Guo XL, Dai ZH, Liu HF, Gong X. An investigation on the heat transfer behavior and slag deposition of membrane wall in pilot-scale entrained-flow gasifier. Fuel 2014;102:491–8.
[30] Seggiani M. Modelling and simulation of time varying slag flow in a Prenflo entrained-Flow gasifier. Fuel 1998;77:1611–21.
[31] Ni JJ, Zhou ZZ, Yu GS, Liang QF, Wang FC. Molten slag flow and phase transformation behaviors in a slagging entrained-flow coal gasifier. Ind Eng Chem Res 2010;49:12302–10.
[32] Zhang BB, Shen ZJ, Han D, Liang QF, Xu JL, Liu HF. Effects of the bubbles in slag on slag flow and heat transfer in the membrane wall entrained-flow gasifier. Appl Therm Eng 2017;112:1178–86.
[33] Ye I, Ryu C. Numerical modeling of slag flow and heat transfer on the wall of an entrained coal gasifier. Fuel 2015;150:64–74.
[34] Ye I, Ryu C, Koo JH. Influence of critical viscosity and its temperature on the slag behavior on the wall of an entrained coal gasifier. Appl Therm Eng 2015;87:175–84.
[35] Yong SZ, Ghoniem AF. Modeling the slag layer in solid fuel gasification and combustion-two-way coupling with CFD. Fuel 2012;97:457–66.
[36] Yong SZ, Gazzino M, Ghoniem AF. Modeling the slag layer in solid fuel gasification and combustion-formation and sensitivity analysis. Fuel 2012;92:162–70.
[37] Xu JL, Liang QF, Dai ZH, Liu HF. Comprehensive model with time limited wall reaction for entrained flow gasifier. Fuel 2016;184:118–27.
[38] Vargas S, Frandsen FJ, Dam-Johansen K. Rheological properties of high temperature melts of coal ashes and other silicates. Prog Energy Combust Sci 2001;27(3):237–429.
[39] Pegoraro PR, Marangoni M, Gut JAW. Residence time distribution models derived from non-ideal laminar velocity profiles in tubes. Chem Eng Technol 2012;35:1593–603.